A Flexibility-based Approach for the Design and Management of Floating Offshore Wind Farms

Samuel Torres-Rincón, Emilio Bastidas-Arteaga, Mauricio Sánchez-Silva

A Flexibility-based Approach for the Design and Management of Floating Offshore Wind Farms

Samuel Torres-Rincón[a,b,*], Emilio Bastidas-Arteaga[b], Mauricio Sánchez-Silva[a]

[a] *Civil and Environmental Engineering Department, Universidad de los Andes, Bogotá, Colombia*
[b] *University of Nantes, Institute for Research in Civil and Mechanical Engineering, CNRS UMR 6183, Nantes, France*

Abstract

Floating offshore wind farms have become a gateway to reach locations that are technically and economically infeasible to exploit using fixed platforms. However, the high capital investments and the uncertainty associated with the reliability, capacity factor, technology evolution, electricity demand, and regulatory frameworks negatively affect the cost of energy of this approach. Alternative strategies, such as designing for flexibility, have been shown to increase the value of engineering systems subject to highly uncertain environments. In this article, an analysis based on life-cycle costs and Monte-Carlo simulation is used to determine if floating wind farms with flexible installed capacity result in lower costs of energy than traditionally designed wind farms. Flexibility is introduced using an adaptable platform strategy and an over-dimensioned platform strategy. The results show that the adaptable platform strategy has the potential to reduce the cost of energy up to 18% by increasing the energy generation and the lifetime of some components of the wind farm. Nonetheless, the benefits of flexibility depend on new legislation that allows for lifetime extensions and proper flexibility management policies that utilize the potential built into the systems.

Keywords: Floating offshore wind generation, Flexibility, Adaptability, Life-cycle analysis, Repowering

1. Introduction

Offshore locations have become a viable option to expand wind energy generation [1, 2] in the last decade. By 2020, the European Wind Energy Association expects to have between 19 and 27 GW installed [3]. However, the costs of building, maintaining, and operating offshore farms are higher than their onshore and close-to-shore counterparts [4, 1] due to the trend of increasing turbine sizes [5] and moving to deeper waters [6, 7, 8, 9] in locations far from shore and difficult access. To facilitate the exploitation of these remote locations, floating platform concepts have been proposed following the example of the oil and gas industry [9]. The main appeal of this concept is that it unlocks locations with water depths greater than 50 m, where bottom-fixed concepts are either technically infeasible or economically unfeasible [1]. However, the capital costs of floating projects can be as large as twice the cost for shallow waters [10]. These additional costs are partially explained by the extra length

*Corresponding author
Email address: sf.torres405@uniandes.edu.co (Samuel Torres-Rincón)

of mooring and export cables required [1], but also by the larger turbines deployed [2] and massive floating platforms. Furthermore, the difficulty to access remote locations increases both operation and maintenance costs due to the need for high-reliability [11].

The expected tendency is that larger and more expensive turbines will be available for farms located further from shore as the industry keeps developing [12]. For instance, a rapid increment in rotor diameter and hub height is reported in [5]. These measures are justified for reports such as [13], where it is stated that increasing the turbine power rating is the technological innovation that has the highest impact on reducing the energy cost. Other authors [14] report that doubling installed capacity can reduce the LCOE between 9 and 17%.

Going far from shore poses the additional challenges of dealing with extreme meteorological conditions that affect the reliability of the grid, increases maintenance costs, and increases turbines' downtime [7]. Möller et al [6] also identified larger uncertainties for far from shore scenarios, which may result in costs underestimation. Further sources of uncertainty related to external social phenomena such as market dynamics, demographic changes, political environment, the evolution of regulatory frameworks, and the development of new technologies pose additional challenges to the management and economic viability of offshore projects. These elements portrait a challenging landscape for offshore floating wind generation: large capital investments and a highly uncertain environment.

These conditions establish the need for innovations and alternative design and management philosophies. The cost reduction effect of increasing installed capacity points towards the implementation of re-powering and lifetime extension strategies. Large costs are not the only challenge faced by floating offshore generation; highly uncertain environments also affect the system output, not only from a technical perspective but also from its perceived competitiveness. If floating offshore generation is to become a viable source of renewable energy, it needs the tools to deal with a complex uncertain environment, which requires going beyond re-powering strategies.

Different authors [15, 16, 17, 18, 19] have identified flexibility and adaptability as key properties to have in engineering systems in the face of uncertainty. These authors associate flexibility with a reduction in the negative impact of uncertainty and even an increased ability to better exploit new conditions. In the context of engineering systems, flexibility is usually defined as the ability of a system to be easily modified [20, 21, 22, 23, 24]. The option for future changes is introduced during the design stage and it is usually coupled with a management policy that suggests when an adaptation should be executed. In the case of wind turbines, flexibility already exists in different components in the nacelle that allow to increase the turbine efficiency and control the operating conditions. However, in this paper we consider flexibility as the option to increase the power rating of the turbines by installing adaptable floating platforms that enable fast replacements.

Although flexibility can be used to achieve re-powering, the concept goes beyond by including specific design measures to enable fast turbine replacement. Furthermore, the concept does not limit its applicability to specific time instants but takes proactive measures in the form of management policies to consider a wide range of external conditions that could motivate an adaptation. However, flexibility does not address problems encountered in re-powering approaches associated with the

financial closure and regulatory compliance of the project.

Developing floating offshore wind farms with flexible capacity could potentially increase the service life and reduce the LCOE. By allowing a fast deployment of larger generators, the wind farm could take advantage of new technologies to increase the installed capacity with reduced production and installation costs. A flexible design and management strategy could improve the competitiveness of operating offshore farms under variable external conditions. For these reasons, this work presents a parametric analysis to evaluate if flexibility is a valuable property for floating offshore wind farms from a life-cycle cost perspective. The results show not only that flexibility can be a desirable property, but also identify the flexibility configurations and management policies that produce the lowest LCOE.

This article is organized as follows: section 2 provides a literature review on the concept of flexibility in the context of engineering systems, section 3 presents the life-cycle cost model used to determine the costs for the baseline and flexible strategies, section 3.3 explains the simulation methodology followed to calculate the LCOE for all cases, and section 4 exemplifies the cost model and simulation methodology in a theoretical farm under multiple scenarios. The results obtained in this section are used to draw conclusions about the impact of flexibility in the cost of energy of floating offshore wind farms.

2. Literature review: flexibility in engineering systems

The concept of flexibility in engineering systems is not considered to be "academically mature" [21] because an exact and commonly agreed definition is yet to be proposed. In this work, flexibility will be understood as defined in [25, 22, 24]: Flexibility is the ability of a system to easily adapt any of its components. The measurement of the effort is generally given in terms of the resources needed to perform the change. It is assumed that an initial investment is required to introduce the option. This additional expenses may come from lengthier design processes and additional materials. It is expected that the size of the initial investments will limit the scope of the adaptations that can be performed through flexibility.

This description of flexibility can be translated into a numerical representation, which can be useful to compare different flexible designs for the same system. This study uses the *flexibility vector* [24] described by Equation 1:

$$\mathbf{f}_i(t) = \left[\frac{c_{nf,i} - c_{f,i}}{c_{f,i}}, \frac{x_{max,i}(t) - x_i(0)}{x_i(0)} \right] \tag{1}$$

This vector describes the flexibility for the design/operational parameter i using two components: the first component measures the resources required to perform an adaptation as the ratio between the unitary cost of modifying i without flexibility $c_{nf,i}$ (without being specifically designed to be adapted); and the unitary cost of performing an adaptation with flexibility $c_{f,i}$. The second component measures the size of the adaptation space as the ratio between the maximum value that i can take and its initial value $x_{max,i}/x_i(0)$. Following this definition, a system's element i can increase its flexibility reducing the adaptation costs or by increasing the adaptation space. The flexibility vector in Equation 1 is

defined for a single design or operation parameter of the system. Depending on the system, multiple flexibility vectors may be needed to describe all adaptation capabilities.

2.1. Flexibility management policies

Designing an engineering system to be flexible is not enough to obtain the reported advantages. The timing and magnitude of the adaptations need to be properly devised to ensure that the system response is optimal [20, 26, 25, 27, 23, 24]. These decisions depend both on technical constraints on the system's performance and specific demands dictated by stakeholders' preferences, regulatory frameworks, and user requirements. These sets of preferences can be modeled using *policies*.

Policies are functions that map a set of system states to decisions [27, 28]. The family and specific parameters of the function allow encapsulating the set of preferences that control the adaptation process. While in some cases the adaptation policies take complex forms to consider risk preferences, for many applications a deterministic policy of the form of "*if-then*" conditionals that trigger an adaptation process [29] is enough to model a wide range of real-life conditions.

The use of policies allows to model the process of managing flexibility as a *sequential decision process* (SDP). The generic SDP model requires an environment and an agent that observes the state $s(t)$ of the environment at time t and selects an action $a(t)$ based on the policy π. At the next time step, a reward $r(t)$ is generated by the environment and received by the agent, while a new state $s(t+1)$ is reached according to a probabilist model. This model combines random elements with the sequence of previous states $s(1:t)$ and actions $a(1:t)$ [30]. Then, the agent observes the new state and selects a new action $a(t+1)$ according to π.

In the case of flexible system management and design, the SDP is applied as follows: First, define the system's initial design properties $x(0)$ and x_{max} (flexibility range of design/operation parameter $x(t)$). Second, define the policy π to guide the adaptation management decisions. Third, during the operation stage, the conditions defined by the policy are monitored to perform an adaptation if needed. This results in a sequence of time instants $\tau_1, \tau_2, \ldots$, and adaptation sizes $y_{\tau_1}, y_{\tau_2}, \ldots$ for all future adaptations. Figure 1 presents a diagram that synthesizes this design and management process.

2.2. Flexibility in offshore floating wind turbines

The concept of flexibility can be applied in different ways to floating offshore wind turbines. In this study two strategies are considered: i) over-dimensioned floating platforms that allow fast installation of new, larger turbines (Strategy A), and ii) floating platforms that are specifically designed to be adapted (expanded) when larger turbines are required and available (Strategy B) (see Figure 2).

While both strategies accomplish the same objective of allowing fast replacement of the wind turbines, Strategy B has higher design costs due to research and development activities required to design adaptable floating platforms. In contrast, production costs are higher for the larger platform of Strategy A due to its larger size. In both cases, however, the mooring and transmission lines are over-designed to restrict the adaptations to the platforms only.

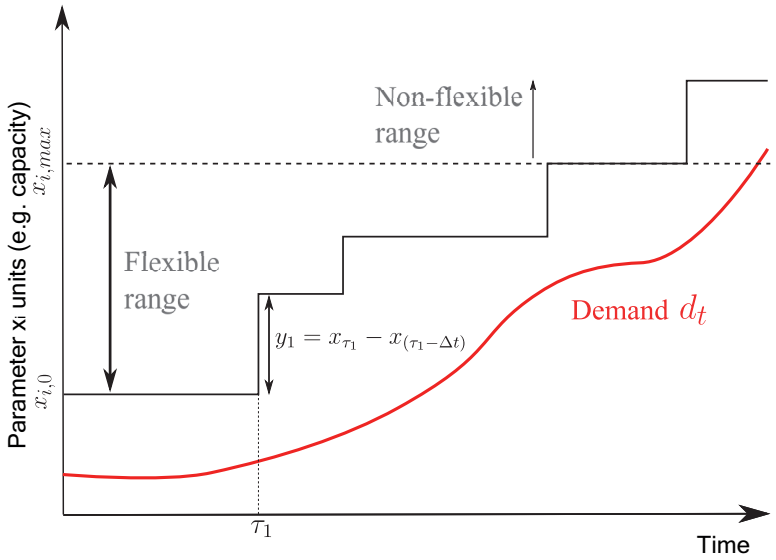

Figure 1: Description of the main elements for flexible designs

When an adaptation is performed, there are additional costs for Strategy B due to the necessary modifications to the platform. The platform from Strategy A has the advantage of allowing an immediate replacement of the turbine. In summary, the difference between strategies is the trade-off between initial and future costs. It is important to remark that the details of the design of the adaptable platform from Strategy B are beyond the scope of this study.

A key element to consider is the type of floating platform. There are three design concepts that commonly appear in the literature: i) semi-submersible platforms (SSPs), ii) spar buoys (SBs), and iii) tension-leg platforms (TLPs). Each platform type has different draft requirements that affect the installation process. While SSPs can be towed from port to the farm site, assembling the turbines with the SBs or TLPs and towing them from port is usually not an option due to the draft requirements for these platforms. The assembly is usually done in deeper waters using floating cranes before the joint turbine and platform can be towed to the site. Furthermore, the SSPs offer a shape more suitable for adaptable modular designs. According to [31, 32, 33], SSPs exhibit the lowest LCOE for a wide range of farm configurations. Assembly can be completed using only a port crane, which is considerably less expensive than using a floating crane. For these reasons, only SSPs are considered in this study.

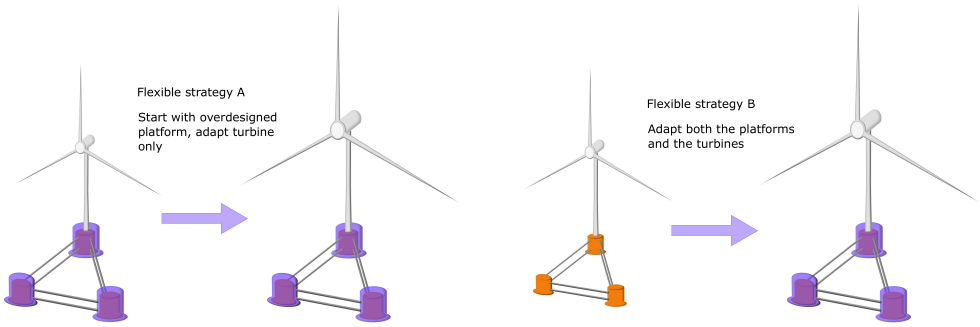

Figure 2: Flexible strategies for floating platform expansions

3. Life-cycle cost model

The evaluation of the economic performance for the flexible strategies is conducted by estimating the Life-cycle Cost of Energy (LCOE) and comparing it with a baseline case with no flexibility. The LCOE is a measure widely used to compare energy generation alternatives by providing an estimation of the average cost of the energy generated.

Estimating these costs for a floating offshore farm is challenging due to the absence of commercial operating farms and the complexity of the systems [2]. The models proposed in [34, 33, 10] provide the best guides available. According to these models, the life-cycle costs of offshore wind farms can be associated with the following stages: i) planning, development, and design; ii) production and installation; iii) operation; and iv) decommissioning.

The planning, development, and design stage costs PDD represent the cost of activities that must be completed before the construction phase such as surveys, development of design concepts, arrangement of legal requirements, and other activities related with project management. These costs are sometimes reported as a unitary price per unit of installed capacity.

The production and material costs, PM, are defined for each component: turbines, floating platforms, mooring and anchoring, and electrical systems. Turbines and platforms costs can be estimated from unitary prices and the capacity of the farm; mooring, anchoring and electrical systems' costs are estimated from a price per unit of length.

Installation costs I depend mainly on farm component, distance from port, and installation procedure. In particular, the installation procedure determines the fleet composition which is a key element in the estimation of I. The next section summarizes the analytical expressions used to estimate these costs.

The operation and maintenance costs, OM, include transmission charges and maintenance activities. The transmission charges are usually represented as a constant amount paid to the government per MWh produced. Maintenance activities can be classified as preventive and corrective. Preventive maintenance costs are represented as a constant yearly cost, while corrective costs depend on the failure rate of individual components [11]. Various authors [8, 35, 12] have found empirical models to calculate these costs as a function of the installed capacity and the distance to shore.

In the case of flexible farms, the operation stage must include the adaptation costs A. For the flexibility strategies discussed in section 2.2 these costs vary as follows: For Strategy A, A are the costs of acquiring and installing the new turbines. For Strategy B, A includes both acquiring and installing new turbines and expanding the platforms. The estimation of these costs is detailed in section 3.2.4.

The costs of decommissioning D include the labor costs, transportation costs, and processing costs [36]. These costs can be partially offset by recycling most of the raw materials. Empirical models in the literature [10] have estimated decommissioning costs as a percentage of installation costs depending on the farm component (turbines, cables, etc.).

Once these costs have been determined, the present value is calculated as:

$$PV_C = PPD + PM + I + \sum_{t=1}^{T} \frac{OM(t) + A(t)}{(1+r)^t} + \frac{D}{(1+r)^T} \tag{2}$$

where T is the planning horizon and r is the discount rate.

3.1. LCOE estimation

To complete the estimation of the LCOE it is necessary to provide a single value to represent the energy generated. The total discounted generated energy PV_E can be calculated using Equation 3.

$$PV_E = \sum_{t=1}^{T} \frac{E(t)}{(1+r)^t} \tag{3}$$

where $E(t)$ is the energy generated in time step t in MWh.

The LCOE is then calculated as the ratio between PV_C (Equation 2) and PV_E:

$$LCOE = \frac{PV_C}{PV_E} \tag{4}$$

3.2. Installation and adaptation costs definition

As discussed at the start of section 3, installation costs I and adaptation costs A depend on farm location, turbine assembly strategy, and transport fleet composition. The estimation of these costs is done using analytical expressions to model the specific conditions. The following sections present the equations adapted from the models published in [2, 33, 10].

Due to the large number of parameters, the following naming convention is adopted: $var_{a,b}$, where var can be any variable from Table 1, and a, b can be physical elements from Table 2 or activities from Table 3. Subscript a represent the direct element or activity measured by var and b is a complement. For instance, $n_{wt,b}$ represents the number of turbines transported per barge, while $n_{b,wt}$ represents the number of barges used to transport turbines.

Table 1: Variables' abbreviations

Symbol	**Name**	**Unit**	**Symbol**	**Name**	**Unit**
I	Installation cost	€	PM	Production and materials cost	€
PDD	Planning, development and design costs	€	OM	Operation and maintenance cost	€
A	Adaptation cost	€	D	Decommissioning cost	€
t	Time	hour	c	Unitary cost	€/unit
d	Distance	m	s	Surface	m^2
l	Length	m	w	Width	m
v	Speed	m/s	n	Number of elements	-
k	Numerical coefficient	-	R	Rate of installation	unit/da
ϕ	Diameter	m			

Table 2: Elements abbreviations

Symbol	Name	Symbol	Name
wt	Wind turbine	fp	Floating platform
tug	Tug	b	Barge
pc	Port crane	fc	Floating crane
a	Anchor	ml	Mooring line
AHV	Anchor handling vehicle	CLV	Cable laying vehicle
ca	Cables	aca	Array cables
eca	Export cables	pp	Platform parts
ofs	Offshore substation	ons	Onshore substation
GIS	Gas insulated switchgear	ts	Transformer
dt	Downtime	p	Port
bl	Turbine blade	tw	Turbine tower

Table 3: Activities abbreviations

Symbol	Name	Symbol	Name
is	Installation on site	ip	Installation at port
tr	Transport	sr	Surface rental
ld	Load into vessel	la	Labor
mo	Mobilization of vessel	lf	Lifting
im	Machinery internal movements	sl	Soil preparation
fd	Foundation	pa	Partial assembling

3.2.1. Wind turbine and floating platform installation costs

The first installation costs considered are for the floating platforms I_{fp}. These costs are estimated assuming specific assembly and transportation procedures for the wind turbine and its platform. The assembly procedure of the wind turbine (tower, rotor, nacelle, and blades) is completed at the port using a crane; then, the full turbine is joined with the floating platform. The joint turbine and platform are loaded into tug vessels to be towed (wet transportation) to the farm site. This transportation method is possible due to the low draft of SSPs [10].

The described installation procedure results in the following costs: port costs $I_{p,fp}$ associated with the storage of turbine and platform components and the use of a port crane to load the assembled turbine into the vessels; transportation costs $I_{tr,fp}$ of using tug vessels, and installation costs $I_{ip,fp}$ associated with the use of the port crane to assemble the turbine and the platform. Therefore, total installation costs for turbines and platforms are [33]:

$$I_{fp} = I_{p,fp} + I_{tr,fp} + I_{ip,fp} \tag{5}$$

Port costs $I_{p,fp}$ are calculated using the following equation:

$$I_{p,fp} = t_{sr,fp}\ s_{fp}\ c_{sr} + n_{wt}\ t_{ld,fp}\ c_{pc} \tag{6}$$

where c_{sr} is the cost of port surface rental ($€/m^2 day$), n_{wt} is the number of wind turbines, and c_{pc} is the cost of port crane rental ($€/hour$). See Appendix A.1 for details on the estimation of these values.

The transportation costs of the platform $I_{tr,fp}$ are defined as:

$$I_{tr,fp} = n_{tug,fp}\ t_{tug,fp}\ c_{tug} + c_{tug,mo} \tag{7}$$

with $n_{tug,fp}$ the number of tugs used per trip, c_{tug} the daily cost of the tug vessel ($€/day$), and $c_{tug,mo}$ its mobilization cost (€).

The installation cost of the turbine and platform at port is:

$$Iip, fp = \frac{t_{ip,fp}}{24}\ n_{wt}\ c_{pc} \tag{8}$$

3.2.2. Anchoring and mooring installation costs

The costs of installing the mooring lines and the anchors $I_{a\&ml}$ are calculated assuming that an Anchor Handling Vehicle (AHV) is used for the task and that both the turbine platforms and the substation platforms use the same number of anchors each.

$$I_{a\&ml} = (c_{AHV} + c_{la,a\&ml})\frac{n_a}{R_{AHV}} \tag{9}$$

where c_{AHV} is the cost of using the AHV ($€/day$), $c_{la,a\&ml}$ are labor costs ($€/day$), and R_{AHV} is the anchor installation rate (per day).

The number of anchors n_a is calculated as:

$$n_a = (n_{wt} + n_{fp,ofs})\ n_{ml,fp} \tag{10}$$

where $n_{fp,ofs}$ is the number of floating platforms for the offshore substation, and $n_{ml,fp}$ is the number of mooring lines per platform.

3.2.3. Electrical systems installation costs

The installation costs of electrical systems are divided into installation of cables I_{ca}, installation of offshore substation I_{ofs}, and installation of onshore substation I_{ons}. The installation costs of cables I_{ca} can be further divided into installation costs of array cables to interconnect the turbines with the offshore substation I_{aca}, export cables that connect the offshore substation with shore $I_{eca,ofs}$, and onshore export cables $I_{eca,ons}$ to reach the onshore substation, as shown by Equation 11:

$$I_{ca} = I_{aca} + I_{eca,ofs} + I_{eca,ons} \tag{11}$$

The installation costs for the array cables I_{aca} are calculated considering the use of specialized vehicles such as Cable Laying Vessels (CLVs) according to Equation 12 [10]:

$$I_{aca} = \frac{c_{CLV,aca}}{R_{CLV,aca}}\ l_{aca} \tag{12}$$

where $c_{CLV,aca}$ is the daily cost of the CLV, and $R_{CLV,aca}$ its installation rate.

The total length of array cable l_{aca} depends on the sea depth, the distance between turbines, and the position of the offshore substation relative to the turbines.

The offshore export cable installation costs $I_{eca,ofs}$ are calculated similarly, but considering that the vessel daily cost $c_{CLV,eca}$ and installation rate $R_{CLV,eca}$ vary due to the difference in cables used:

$$I_{eca,ofs} = \frac{c_{CLV,eca}}{R_{CLV,eca}}\ l_{eca,ofs} \tag{13}$$

with $l_{eca,ofs}$ the length of offshore export cable (m).

The onshore cable installation costs $I_{eca,ons}$ are calculated as:

$$I_{eca,ons} = c_{eca,ons}\ l_{eca,ons} \tag{14}$$

where $c_{eca,ons}$ is the unitary price of cable installation (€$/m$) and $l_{eca,ons}$ is distance between shore and the onshore substation (m).

The installation costs for the offshore substation I_{ofs} are estimated similarly as in the case of the wind turbines, considering port costs $I_{p,ofs}$, transportation costs $I_{tr,ofs}$, and on-site installation costs $I_{is,ofs}$ [33, 10]:

$$I_{ofs} = I_{p,ofs} + I_{tr,ofs} + I_{is,ofs} \tag{15}$$

The port costs $I_{p,ofs}$ consider the hiring of the port surface to store the transformers and floating platforms s_{ofs} until they are loaded to be transported, and the rental of the port crane to load the parts into the vessels, as shown by Equation 16 [33]:

$$I_{p,ofs} = t_{sr,ofs}\ s_{ofs}\ c_{sr} + (n_{ts} + n_{fp,ofs})\,(t_{ld,ts} + t_{ld,fp})\ c_{pc} \tag{16}$$

with n_{ts} the number of transformers. The expressions to estimate these values are presented in Appendix A.2.

The transportation costs for the offshore substation are calculated as:

$$I_{tr,ofs} = (n_{b,ofs}\ t_{b,ofs}\ c_b) + (n_{tug,ofs}\ t_{tug,ofs}\ c_{tug}) + c_{b,mo} + c_{tug,mo} \tag{17}$$

where $n_{b,ofs}$ and $n_{tug,ofs}$ are the number of vessels in the operation.

Finally, the installation costs are estimated as:

$$I_{is,ofs} = t_{fc,ofs}\ c_{fc} + c_{fc,mo} \tag{18}$$

with c_{fc} and $c_{fc,mo}$ the daily rate and the mobilization cost of the floating crane.

The installation costs for the onshore substation I_{ons} are estimated using Equation 19 [33]:

$$I_{ons} = I_{sl,ons} + I_{fd,ons} + I_{is,ons} \tag{19}$$

with $I_{sl,ons}$ the costs of preparing the soil, $I_{fd,ons}$ the cost of the foundation, and $I_{is,ons}$the cost of installation.

3.2.4. Adaptation costs

The costs of performing an adaptation depend on the flexibility strategy, as described in section 2.2. For Strategy A, the adaptation costs correspond to the acquisition costs of the new turbines plus the installation costs. In this case, the installation procedure differs from the process followed during the farm construction. The turbines cannot be fully assembled and towed, and instead, they are transported in parts using a barge. Parts of the turbine may be partially assembled at port. The installation at sea is conducted using a floating crane to dismount the old turbines and install the new devices on the existing platforms. The use of floating cranes comes from the assumption that minimizing the adaptation times is the priority. For an alternative objective, a different procedure, such as towing the platforms back to port, could be proposed.

The costs for this installation procedure can be divided in port costs A_p, transportation costs A_{tr}, and installation costs A_{is}, as described by Equation 20:

$$A = A_p + A_{tr} + A_{is} \tag{20}$$

Port costs A_p consider the rental of storage area at the port and the use of a port crane to load the turbine into the transport vessel:

$$A_p = t_{sr,wt}\ s_{wt}\ c_{sr} + n_{wt}\ t_{ld,wt}\ c_{pc} \tag{21}$$

See Appendix A.3 for details on the estimation of these values.

The transportation costs A_{tr} using a barge vessel are defined in Equation 22.

$$A_{tr} = n_{b,wt}\ t_{b,wt}\ c_b + c_{mo,b} \tag{22}$$

The installation costs A_{is} are divided between the preassembly costs using the port crane and the offshore installation costs using a floating crane, according to Equation 23:

$$A_{is} = t_{fc,wt}\ c_{fc} + c_{fc,mo} + 24\ t_{pc,pa}\ c_{pc} \tag{23}$$

For the case of Strategy B, a slightly different adaptation procedure is followed. This strategy requires the transportation and installation of floating platform expansion elements besides the new turbines. While Equations 20-23 are valid, a few modifications are needed in the number of lifting movements to consider the additional elements that must be loaded, transported, and installed.

Specifically, $n_{li,wt}$ in Equation A.15 and $n_{li,is}$ in Equation A.18 must be increased by the number of platform adaptation parts n_{pp}. The number of devices transported per barge vessel $n_{wt,b}$ in Equation

A.14 also has to be adjusted to account for the additional space on deck required to place the platform parts.

3.3. Simulation Methodology

The purpose of the cost model presented in previous sections is to evaluate the impact of flexibility in the economical performance of floating offshore wind farms under uncertain demand, technology prices, and capacity factor. For this purpose, a Monte-Carlo simulation procedure, described in Figure 3, was developed.

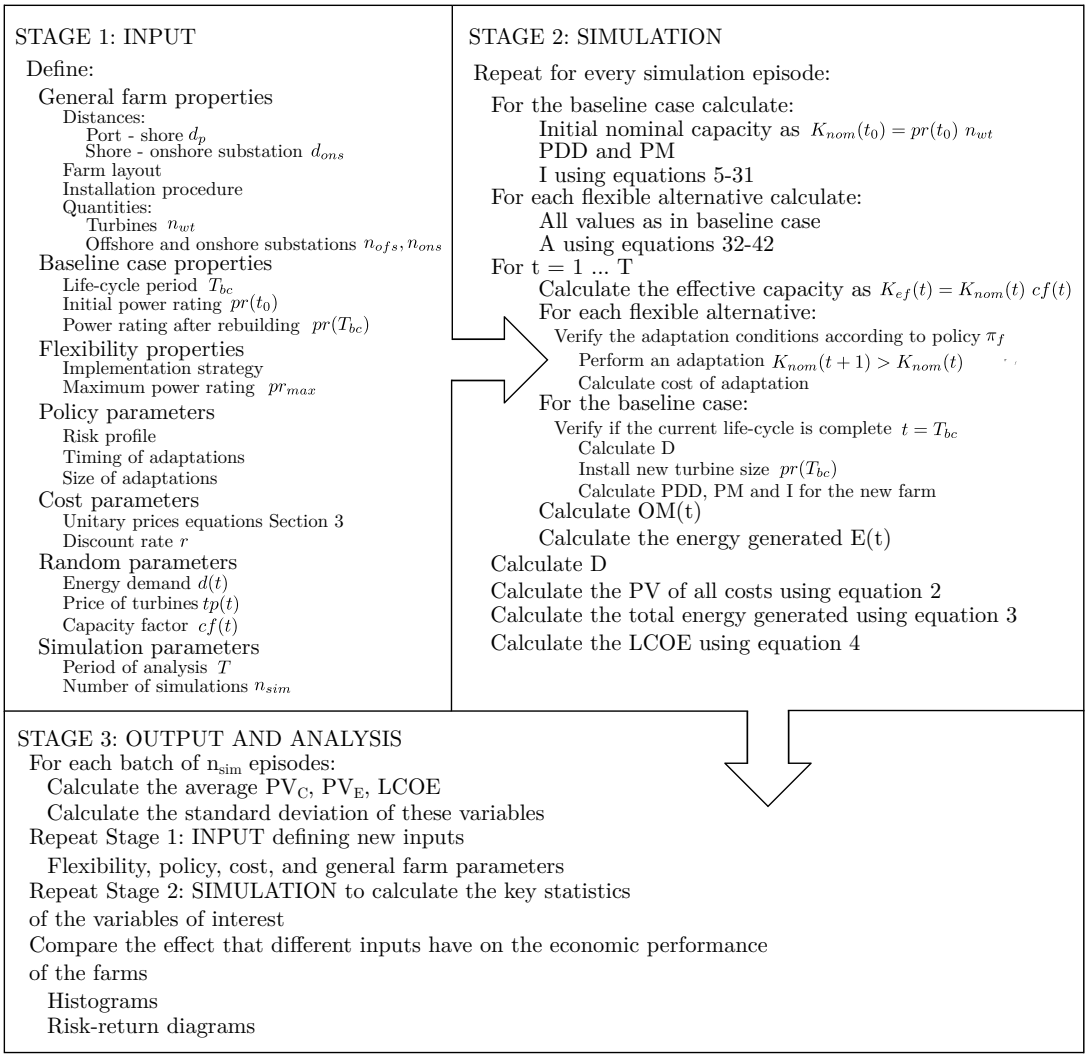

Figure 3: Stage 1: Input

The procedure consists of 3 stages: Definition of input parameters, simulation, and output analysis. In the first stage, as shown by Figure 3, the parameters that characterize the farm, the costs, the random processes and the policy are defined together with the meta-parameters of the simulation. During the second stage, multiple trajectories of the random processes are simulated, and the discounted life-cycle costs and energy generated are calculated for the different system responses. In the third stage, the average LCOE is estimated for the batch of data from the second stage and

conclusions are drawn by comparing the results for the flexible and baseline cases. This procedure is repeated for each farm configuration, flexibility strategy, and flexibility policy to be analyzed.

The computational implementation of this methodology can be performed using algorithms of order $O(n)$. The independence between runs encourages the use of parallel computing to reduce processing times. An implementation in Matlab® 2017b using an Intel®Core™ i5-5200 2.20GHz processor takes 15 seconds in average to run one batch of 1000 simulations.

4. Numerical Example

The life-cycle cost model presented in section 3 and the simulation procedure presented in section 3.3 are tested using a generic farm. Five cases are considered: flexible Strategy A (i), B (ii), a baseline case (iii), a case with no re-powering (iv), and a re-powering case with no decision flexibility (v). The flexible strategies are described in section 2.2. The baseline case represents a wind farm without flexibility, which is rebuilt once in the middle of the planning horizon. This includes removing all installed components including mooring lines and transmission cables. The case with no re-powering is similar to the baseline case but the farm is never rebuilt. The last case also has over-designed platforms, as in case (i), but the adaptation is always conducted in the middle of the planning horizon. When the the farm is rebuilt or re-powered, the new installed capacity is defined by a required demand/capacity ratio.

The planning horizon is defined as $T = 50$ years to allow the comparison of the flexible strategies with two life-cycles of cases (iii) and (v), which are assumed equal to 25 years each [36]. Case (iv) remains unchanged during the entirety of T. The farm location is defined at 100 km from shore (where the port is also located), but a sensitivity analysis of this parameter is considered. Similarly, the initial average sea depth is 100 m but other depths are addressed in the sensitivity analysis. The farm has 100 units with identical power rating, arranged in a grid pattern of 10×10 units (see Figure 4). The average distance between units is 7 times the initial turbine diameter. The electrical systems are composed of one substation offshore and one onshore. The offshore substation is located in the center of the grid (Figure 4), while the onshore substation is located 5 km inland. Wake and electrical losses are assumed constant.

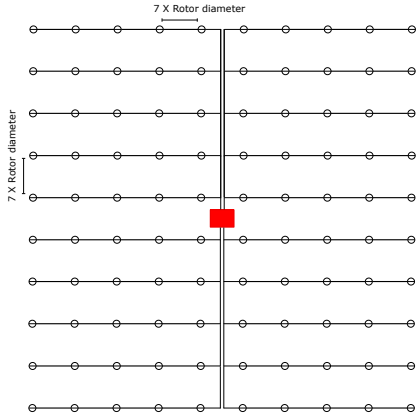

Figure 4: Farm Layout

Table 4: Costs of planning, development, design and production of turbines and platforms

Source and values of various unitary prices					
PM_{fp} (€/MW)			Source [10]		Average
			1 274 900		1 274 900
PDD (€/MW)	Source [1]	Source [2]	Source [8]		Average
	210 000	577 900	280 600		356 167
PM_{wt} (€/MW)	Source[1]	Source[2]	Source[8]	Source [12]	Average
	1 300 000	1 197 468	1 581 342	1 305 600	1 348 602

Table 5: Mooring and anchoring production costs

	Cost component	Value
Mooring	Length per turbine	900 m
	Total length	90 000 m
	Steel density	177 kg/m
	Total steel mass	15 930 000 kg
	Unitary steel mooring price	7.92 €/kg
Anchoring	Anchors per turbine	6
	Anchor weight	3150 kg
	Total anchor mass	1 980 900 kg
	Unitary steel anchoring price	2 €/kg

The cost parameters used to calculate the general costs described in section 3 are presented in the following section. These cost parameters were obtained from multiple sources in the literature.

4.1. Cost estimation

The first cost parameters considered are planning, development, and design costs PDD; turbine production costs PM_{wt}; and floating platform production costs PM_{fp}. These costs are generally reported as unitary prices in €/MW or converted using the rate of exchange of the year of the report and adjusting it by the inflation of 2019. In this example, these costs are estimated as the average unitary price of multiple sources, as shown in Table 4.

In contrast, the mooring and anchoring production costs PM_a, PM_{ml} are estimated using a unitary price for the amount of steel required. Therefore, the total costs will depend on the number of anchors per turbine, the length of each mooring line, the density of the steel used, and the unitary price of the steel. The length of each mooring line is defined as 1.5 the average water depth. It is also assumed that 6 mooring lines are used for each wind turbine. Table 5 summarizes these parameters for depths of 100 m [10].

The production costs of electrical cables PM_{aca}, PM_{eca} are estimated based on a price per unit

Table 6: Electrical systems costs

Cost component	Value
Unitary price array cables	279 €/m
Unitary price export cables HVDC	336 €/m
Offshore substation	$0.11 \cdot n_{wt} p_r \cdot 1E6$
Onshore substation	0.5 Offshore substation cost

of length for each type of cable. The length of the inter-array cables is calculated using the layout from Figure 4 assuming that the cables are installed on the seabed. At the midpoint of each row of the grid, the cables are directed towards the offshore substation. The production costs of the offshore and onshore substations PM_{ofs}, PM_{ons} are estimated using an empirical function of the installed capacity found in the literature [10]. Table 6 presents these costs.

Installation costs for all farm components are calculated using the analytical expressions from sections 3.2.4 - 3.2.3 and the parameters in Table 7 [33, 10].

The costs for the adaptation process are divided between production costs and installation costs. Production costs correspond to the costs of new turbines, offshore and onshore substations, and, in the case of Strategy B, the floating platform expansion elements. Turbine costs are calculated using the prices in Table 4 and the stochastic processes from section 4.2. The costs of the substations are estimated using Table 6.

The operation and maintenance costs OM are generally reported in the literature as a function of both the installed capacity and the farm location. In this study, a linear approximation as a function of the distance to port is considered, for costs ranging between 110 000 and 130 000 €/MW/year. These values were estimated from recent reports in the literature [8, 35, 12].

Finally, the decommissioning costs are estimated as a percentage of installation costs plus an additional charge for site cleaning that depends on the farm area. Theses percentages depend on the element, as shown in Table 8 [1].

4.2. Stochastic parameters

The simulation process considers the effect from three random processes as described in section 3.3: demand $\delta(t)$, technology (turbine) price $tp(t)$, and capacity factor $cf(t)$. These processes are simulated as time series with shapes and tendencies that follow historical data or predictions reported in the literature. For instance, the demand process is generated according to Equation 24:

$$\delta(t) = \max\left\{\beta_1 t + e^{\beta_2 t}\ \beta_3\ \sin(\beta_4 t)\ t + \beta_5 + B(t)\ t, 0\right\} \tag{24}$$

where β_1 to β_5 are normally distributed random variables and $B(t)$ is a Wiener process [37]. The values of these variables used in the example are presented in Table 9. The function $\delta(t)$ allows to simulate a demand tendencies similar to the curves of the prediction models reported in [38, 39, 40]. While

Table 7: General cost parameters

Parameter	Value	Unit	Parameter	Value	Unit
$I_{fd,ons}$	312 000	€	$n_{fp,tug}, n_{fp,ofs}$	1	platforms
$I_{is,ons}$	63 500	€	$n_{fc,wt}$	1	vessels
$I_{sl,ons}$	660 000	€	tip, fp	3	hours
c_{AHV}	48 860	€/day	$n_{li,fp}$	6	lifts
c_b	35 000	€/day	$n_{li,ofs}$	4	lifts
$c_{CLV,aca}$	91/000	€/day	$n_{li,wt}$ Strategy A	5	lifts
$c_{CLV,eca}$	114/000	€/day	$n_{li,wt}$ Strategy B	8	lifts
c_{pc}	833.33	€/$hour$	$n_{li,is}$ Strategy A	10	lifts
c_{fc}	116 000	€/day	$n_{li,is}$ Strategy B	13	lifts
$c_{eca,ons}$	600	€/m	$n_{li,pa}$ Strategy A&B	2	lifts
$c_{la,a\&ml}$	5 656	€/day	$n_{ml,fp}$	6	mooring lines
$c_{b,mo}$	0	€	n_{pp}	3	parts
$c_{fc,mo}$	150 000	€	n_{ts}	3	transformers
$c_{tug,mo}$	0	€	$n_{tug,fp}$	2	vessels
c_{sr}	0.02	€/m^2 day	$n_{tug,ofs}$	1	vessels
c_{tug}	22 502	€/day	n_{wt}	100	turbines
ϕ_{bl}	0.5	m	$R_{CLV,aca}$	150	m/day
ϕ_{tw}	6	m	$R_{CLV,eca}$	200	m/day
d_p	100	km	R_{AHV}	7	anchors/day
k_{dt}	0.75	-	r	3%	-
l_{bl}	61.5	m	$t_{im,fc}$	8	hours
$l_{eca,ons}$	5000	m	$t_{li,fp}, t_{li,ofs}, t_{li,ts}, t_{li,wt}$	3	hours
l_{fp}	76	m	$t_{li,is}, t_{li,pa}$	3	hours
l_{GIS}	4	m	v_b	3.6	m/s
l_{ts}	6.3	m	v_{fc}	3.14	m/s
n_a	6	anchors	v_{tug}	3.6	m/s
$n_{b,ofs}, n_{b,wt}$	1	vessels	w_{ts}	5	m
$n_{ts,b}$	3	transformers	w_{GIS}	2.5	m
$n_{wt,b}$ Strategy A	6	turbines	$n_{wt,b}$ Strategy B	4	turbines

there is a general linearly increasing tendency, there are local oscillations that simulate medium-term variability. The addition of the Wiener process allows to model short-term variability, with uncertainty increasing in time. Figure 5a shows instances of the demand trajectories generated by Equation 24.

Similarly, the technology (turbine) price process is generated using Equation 25:

Table 8: General cost parameters

Decommissioning item	Percentage of installation costs / Unitary price
Turbine and platform	70%
Electric cables	10%
Substations	90%
Mooring lines anchoring	90%
Site cleaning	56400 €/km^2[10]

Table 9: Random demand process parameters

Parameter	Distribution(μ, σ^2)
β_1	$\mathcal{N}(20, 6)$
β_2	$\mathcal{N}(-0.02, 0.006)$
β_3	$\mathcal{N}(10, 3)$
β_4	$\mathcal{N}(0.5, 0.15)$
β_5	$\mathcal{N}(150, 45)$

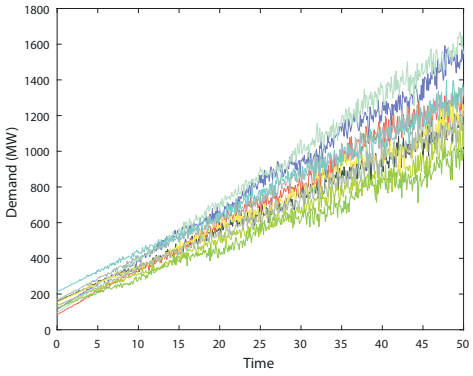

(a) Demand process realizations

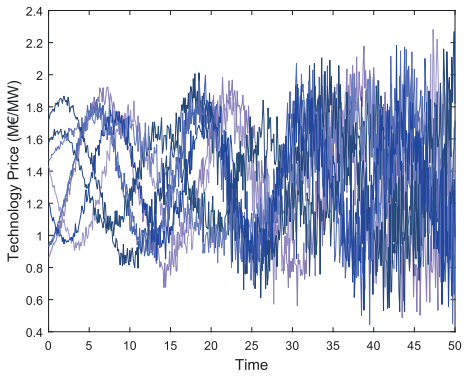

(b) Turbine price process realizations

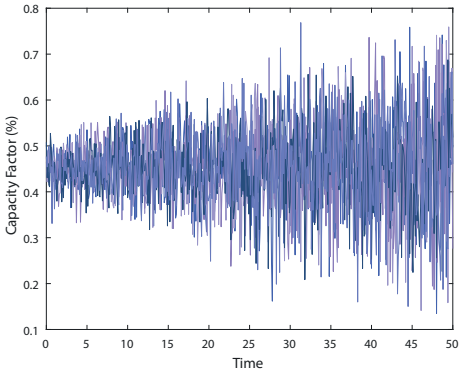

(c) Capacity factor process realizations

Figure 5: Examples of the random processes

$$tp(t) = \max\{\beta_1 \ \sin(\beta_2 t + \beta_3) + \beta_4 + B(t)\ t, 0\} \tag{25}$$

where β_1, β_2, are normally distributed random variables, β_3 is uniformly distributed, and β_4 is a constant calculated as the average turbine prices reported in Table 4, and $B(t)$ is a Wiener process. Table 10 presents the parameters of these variables used in the example. The function represents an oscillating trajectory according to the historical data shown in [41]. The oscillating behavior is justified by the variable price of the raw materials, which represent a considerable portion of the total turbine prices. Figure 5b shows instances of the trajectories generated using Equation 25.

Table 10: Random turbine price process parameters

Parameter	Distribution(μ, σ^2)
β_1	$\mathcal{N}(400000,\ 120000)$
β_2	$\mathcal{N}(0.4,\ 0.12)$
β_3	$\mathcal{U}[0, 2\pi]$
β_4	1348602

Finally, the capacity factor, which determines the effective capacity of the farm, is simulated as a random process according to the following equation:

$$cf(t) = \max\{\beta_1 \ \sin(\beta_2 t)\ t + \beta_3 + B(t)\ t, 0\} \tag{26}$$

where β_1, β_2, are normally distributed random variables, β_3 is an average capacity factor, and $B(t)$ is a Wiener process. Again, the parameters of the variables used in the example are summarized in Table 11. Function $cf(t)$ represent a rapidly oscillating tendency between typical values reported in the literature [42, 43, 44]. The increment in the uncertainty over time is a modeling decision that attempts to capture the difficulty of predicting for such long time periods. In this case, this variability may come from the evolution of environmental conditions, technological evolution of the turbines, and the improvement in the knowledge of the operation. Figure 5c shows instances of capacity factor trajectories generated by Equation 26.

Table 11: Random capacity factor process parameters

Parameter	Distribution(μ, σ^2)
β_1	$\mathcal{N}(5 \times 10^{-4},\ 1.5 \times 10^{-4})$
β_2	$\mathcal{N}(0.7,\ 0.21)$
β_3	0.45

4.3. Flexibility policy

The flexibility management policy π_f discussed in sections 2.1 and 3.3 can be formulated for this example using two functions: First, function $P : \mathbb{R}X\mathbb{R}X\mathbb{R} \rightarrow 0, 1$ maps the triplet $(\delta(k), tp(k), cf(k))$

at time instant $t = k$ to a value in the interval $[0, 1]$. The second function, $Q : [0, 1] \rightarrow 0, 1$, takes the output of function P and produces a decision: 1 to perform an adaptation and 0 to do nothing. This function requires an input parameter to define this decision threshold, the *adaptation trigger* AT.

Every time an adaptation decision is triggered, a second parameter, the *desired performance after adaptation*, PAA, determines the turbine size to be installed based on the ratio demand/effective capacity required after an adaptation is completed. This procedure is repeated until the installed flexibility is depleted. Adaptations outside the flexibility range are not considered in the example.

4.4. Results of simulation scenarios

The results presented in this section are the outcome of 1000 simulation episodes generated for a single set of wind farm configurations and management policy parameters. For each episode and set of parameters an installed capacity profile is obtained, as shown in Figure 6. Each episode consists of 501 time steps, which means that the conditions of the decision process are evaluated 10 times per year for the simulation period of 50 years.

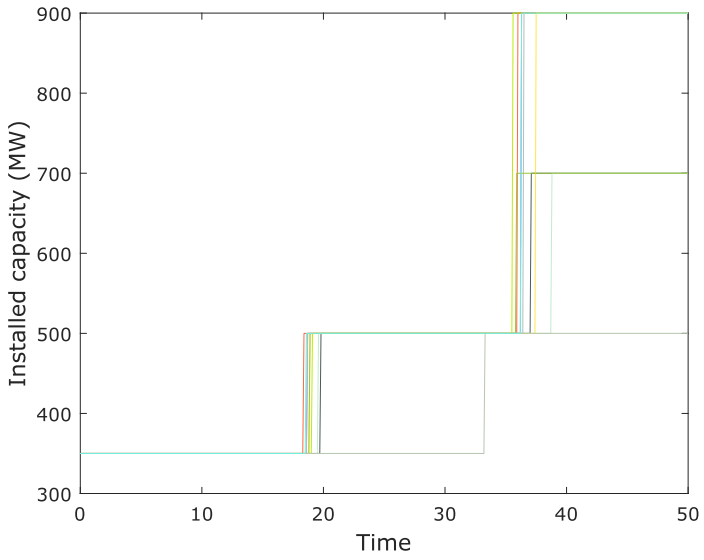

Figure 6: Installed capacity evolution

Each capacity profile is paired with a sequence of investments that occur at different time instants. For instance, all the initial investments (PDD, PM, and I) are assumed as a punctual investment occurring at the first time step. In contrast, the operation and maintenance costs $OM(t)$ are calculated as a sequence of investments uniformly distributed over the simulation period. Adaptation costs $A(t)$ are punctual investments that occur at variable time steps. Instances of the adaptation costs profiles are presented in Figure 7.

The profiles presented in Figures 6 and 7 show that the flexible strategies result in adaptations every $\sim$ 18 years, in contrast with the single reconstruction in year 25 for the baseline case. This adaptation frequency and the magnitude of the increments are the result of the policy defined (section 4.3) and the available flexibility.

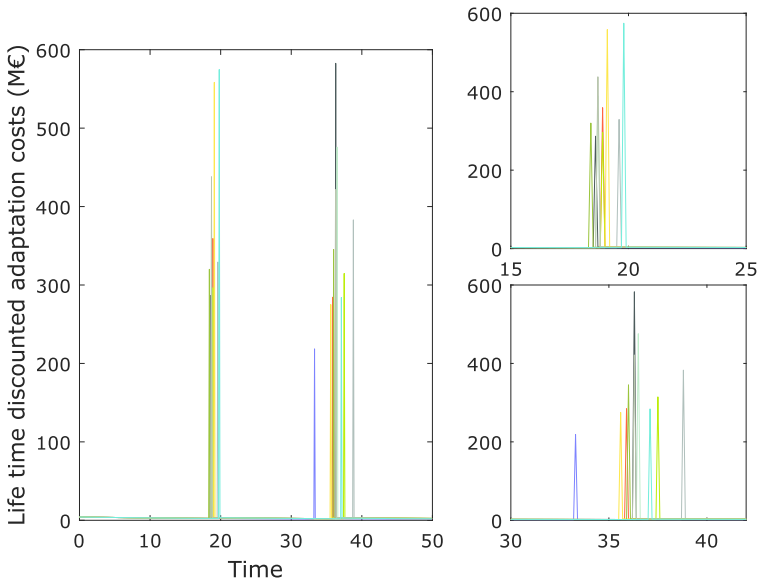

Figure 7: Evolution of discounted adaptation costs

The sensitivity analyses presented in the following sections explore the effect that various parameters related to the implementation of flexibility in floating wind farms have on the LCOE.

4.4.1. Size of flexibility space

The first analysis evaluates the impact of the flexibility range on the LCOE. The flexibility range of Equation 1 corresponds to the maximum turbine power rating allowed by the floating platform designs, following either Strategy A or B. The initial power rating is assumed as 8 MW for both flexible strategies and the baseline case. The maximum turbine power rating allowed by flexibility can be [10 12 15 18 20] MW. When a maximum power rating larger than 8MW is selected, the system has access to all intermediate sizes. All sizes are available to rebuild the baseline case at $t = 25$ years while case (v) has the same limit as Strategy A.

Figure 8 shows the average LCOE as a function of the flexibility range. The average LCOE values vary between 65 and 95 €/MWh, which is similar to the values described in the most recent technical reports [43, 44]. It can be observed that the lowest LCOE is produced by the unchangeable system (case (iv)) followed by Strategy B and the baseline case. This suggests that the cost of replacing the turbines is too large and is not compensated by the additional energy produced. However, case (iv) provides a bound rather than a realistic alternative because it may be too optimistic to assume that a wind farm can operate for 50 years without at least one major replacement.

Figure 8 also shows that both flexible strategies and re-powering case (v) result in lower LCOE compared with the baseline case for maximum power ratings up to 15 MW. Beyond that point, implementing flexibility using Strategy A becomes overly expensive, while Strategy B slowly loses its advantage over the baseline case. The difference in slopes between Strategy A and B shows the large impact that expensive flexibility-introduction measures have on the overall economical performance of the farm. Strategy B is competitive because it can take advantage of low turbine prices, as Strategy A, with a lower initial investment. Case (v) follows the same trajectory as Strategy A, but the difference

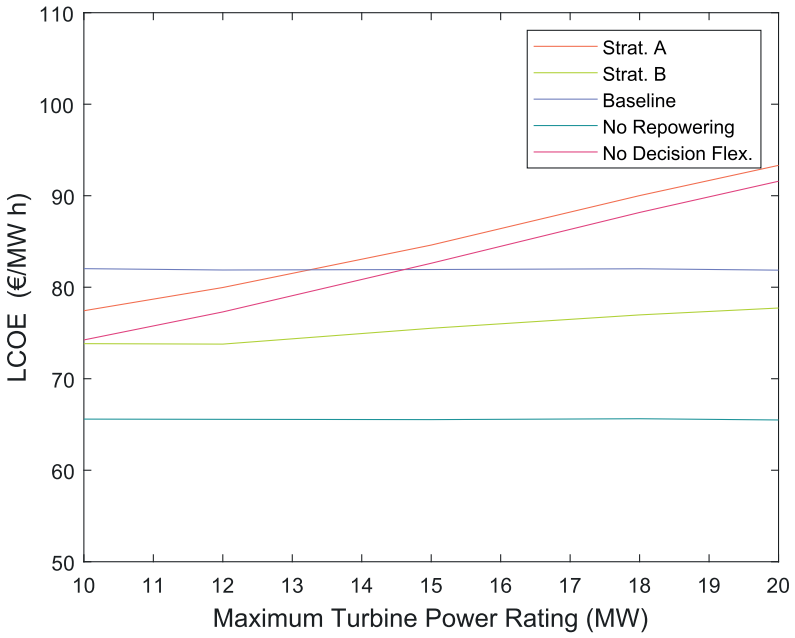

Figure 8: Average LCOE for variable maximum flexible range

in the adaptation timing creates a small gap due to discounting.

Besides the increased cost, the flexible strategies suffer from stagnation in the energy generated, as shown in Figure 9. This figure shows that the flexible strategies are able to generate more energy than all the other options, but the asymptotic behavior observed in both strategies suggests that the external conditions are not sufficient to justify the investments required for the largest flexibility ranges, and this is reflected in the larger LCOE. This highlights the fact that the value offered by flexibility not only depends on the design properties but also on the management policy and the external conditions.

4.4.2. Policy parameters

The results from the previous experiment offered a glimpse of the importance of the flexibility management policy. For this analysis, the management policy is defined as described in section 4.3, using two parameters: the adaptation trigger AT and the desired performance after adaptation PAA. The first parameter influences the timing of the adaptations while the second parameter affects the magnitude of the change. An AT close to 1 represents an insensitive policy that requires extreme conditions to decide to perform an adaptation. A PAA close to 1 represents a policy that prefers large adaptations, as much as the installed flexibility allows it.

Figure 10 shows the LCOE as a function of the AT for turbines with maximum power rating of 20 MW and initial power rating of 8 MW. Increasing AT decreases the LCOE for both flexible strategies, while cases (iii)-(v) are unaffected. Larger AT result in systems that are adapted less frequently by increasing the tolerance to external changes. This results in lower adaptation costs, but also in less energy produced, as can be observed in the energy curve from Figure 11. The sharper fall experienced by both flexible strategies between $AT = 0.35$ and $AT = 0.4$ suggests that for lower

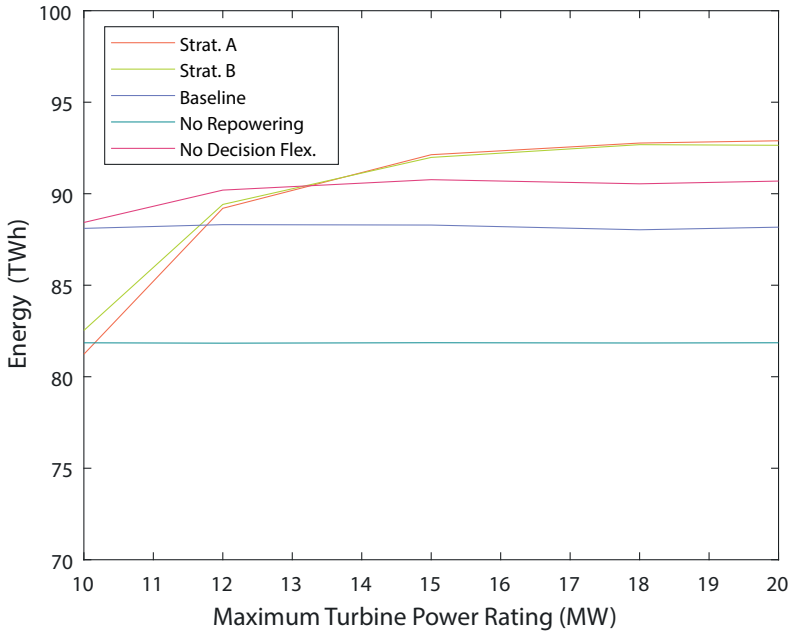

Figure 9: Average discounted energy generated for variable maximum flexible range

values the system is sensitive enough to demand an additional adaptation.

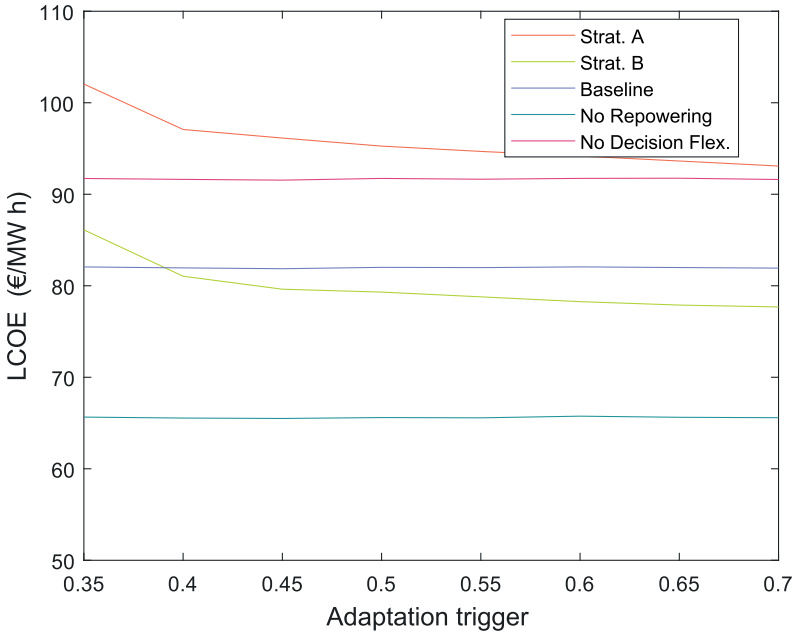

Figure 10: Average LCOE for variable AT

The PAA has a smaller impact on the LCOE for the flexible strategies (see Figure 12). This parameter also affects the baseline case and re-powering case (v) because it defines the new size when the system is rebuilt, re-powered, or adapted. Increasing the PAA results in larger and more expensive adaptations, increasing in consequence energy generation as shown by Figure 13. However, the small change in the LCOE suggests that the considerable increment in energy generated barely

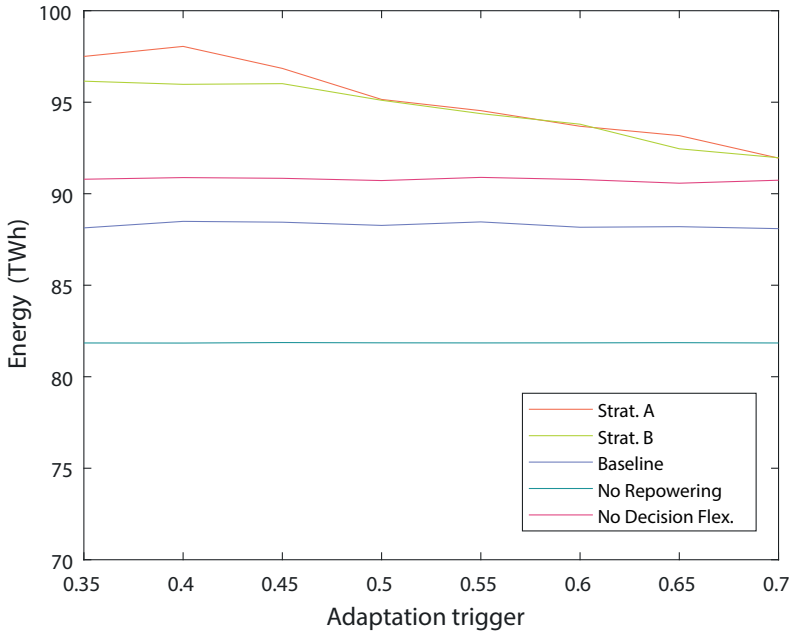

Figure 11: Average discounted energy generated for variable AT

offsets the extra costs of adding and using flexibility.

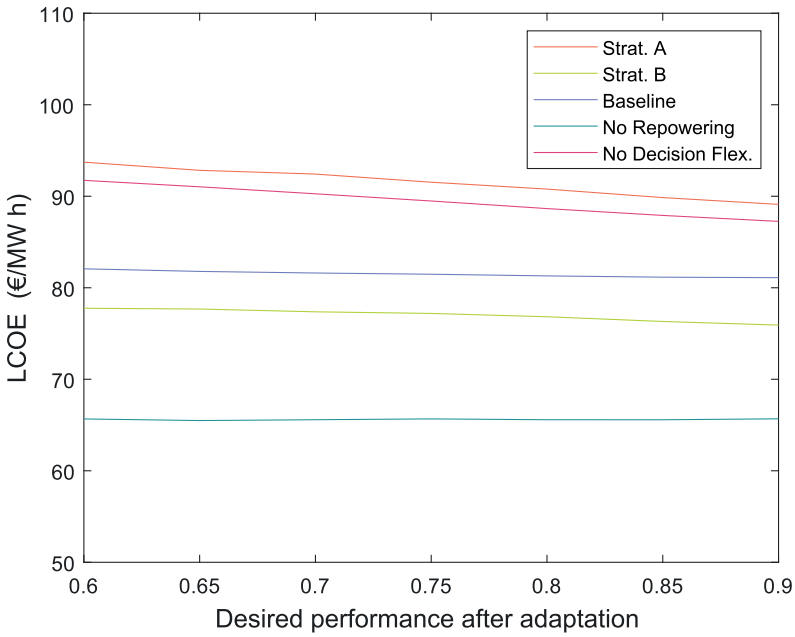

Figure 12: Average LCOE for variable PAA

4.4.3. Initial design

To explore in more detail the design space, in this section the initial turbine power rating is variable taking values between 6 and 18 MW, while the maximum power rating is kept at 20 MW. Figure 14 shows how the average LCOE changes for all cases by increasing the initial design. It is

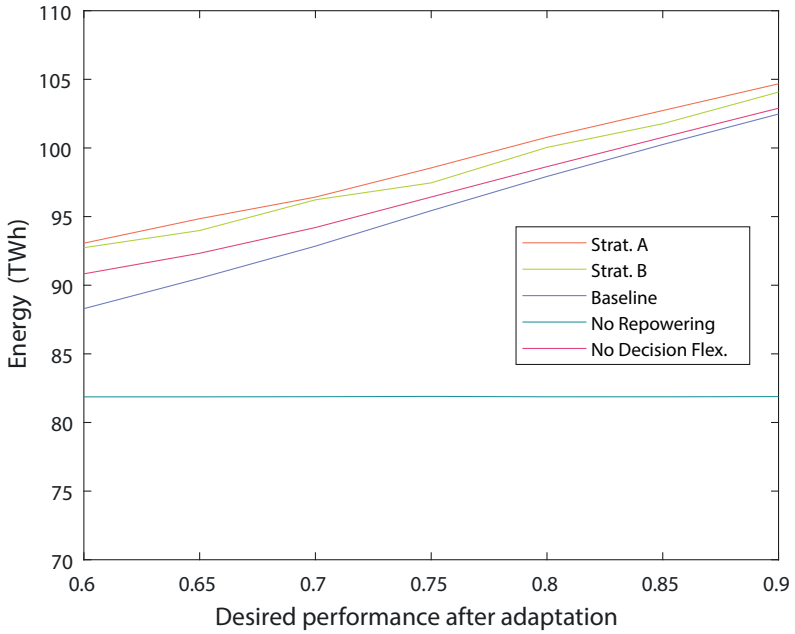

Figure 13: Average discounted energy generated for variable PAA

interesting to observe that both flexible strategies converge to the same point, approaching the no re-powering case (iv). In contrast, the baseline case remains almost constant. By increasing the initial design, the flexible strategies may not require adaptations, behaving as case (iv). Cases (iii) and (v) are always modified, but the costs in case (iii) are larger.

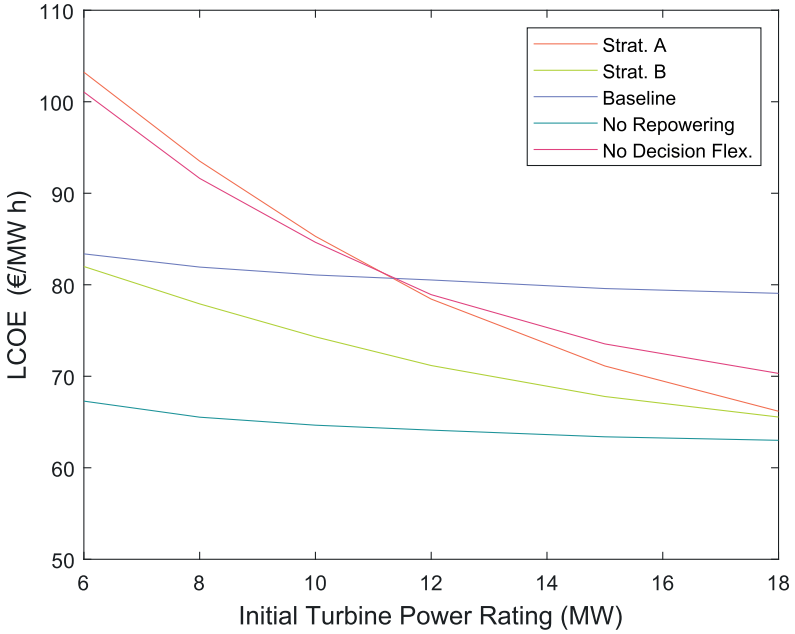

Figure 14: Average LCOE for variable initial turbine rating

These results are in line with previous reports (e.g. [13]) that establish that the most impactful way to reduce the LCOE in offshore wind is to increase the turbine power rating. Nonetheless, this

policy is not definitive as the capital costs can be prohibitive for many projects, even if there is a considerable reduction in LCOE.

4.4.4. Distance from port

In this section, the effect of flexibility on the LCOE is evaluated considering the distance between port and the farm d_p. It is assumed that the port is located at the nearest shore, and that the water depth increases linearly with the distance from shore. The flexible strategies have a maximum power rating of 20MW.

Previous studies showed the correlation between LCOE, water depth, and distance from shore, due to larger mooring and export cable costs [1, 5]. Distance also increases installation and adaptation costs, OM costs, and decommissioning costs. Figure 15 shows the LCOE curve for the following set of distances: $[20, 30, 40, 50, 100, 150, 200]$ km. The flexible strategies exhibit an 6% increment when going from 50 to 100 km, and an increment of 12% when going from 100 km to 200 km, which is similar to the 11% increment by doubling the distance reported in [2].

The baseline case seems to grow faster than Strategy B up to 150 km. While the adaptation costs are slightly affected by the increment in transportation costs, the mooring and electric cables costs have a considerable impact on the costs of rebuilding the farm in the baseline case.

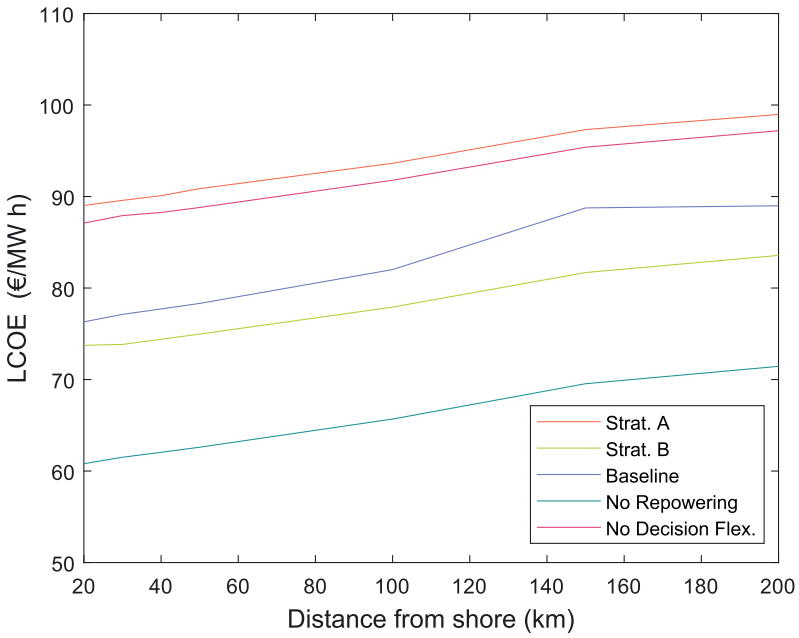

Figure 15: Average LCOE for variable farm location

4.4.5. Discount rate

To conclude the parametric analysis, this section compares the effect of the discount rate on the average LCOE. In all the previous analyses a value of 3% was used considering the long time horizon [45]. Nonetheless, it is of interest to observe how the discount rate affects the economical performance of the alternatives.

Figure 16 presents the average LCOE of the 5 scenarios for discount rates between 3% and 10%. Strategy A and the re-powering case exhibit the largest increment in LCOE (2X) due to their relatively large capital costs and the less valuable discounted energy. From 5%, Strategy B becomes more expensive than the baseline case as the future benefits of flexibility becomes less and less valuable in comparison with the initial investment required to add flexibility.

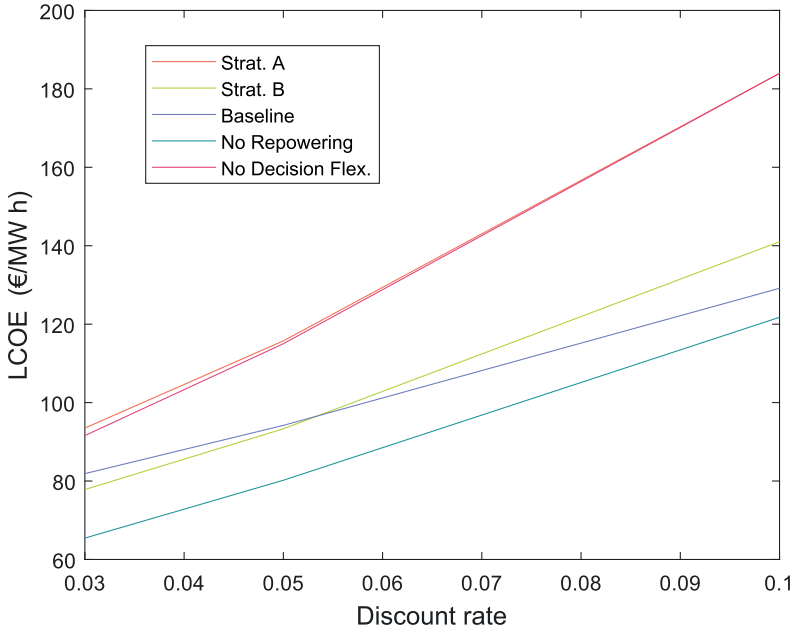

Figure 16: Average LCOE for variable discount rate

4.4.6. Comparison of flexible strategies and management policies in the Risk- Return space

The previous comparisons between flexibility ranges and management policies can be summarized in the risk-return space. The risk-return space is used in financial applications to compare portfolios [46]. This tool can be adapted to evaluate the performance of real assets. In this case, the return is replaced by the average LCOE and the risk by the standard deviation of 1000 simulations of the same wind farm configuration and management policy. The result is Figure 17 where each point corresponds to one of the five scenarios with the wind farm located 100 km from shore/port, with initial turbine power rating between 6 and 18 MW, with maximum power rating between 8 MW and 20 MW, managed with AT between 0.35 and 0.75 and PPA between 0.5 and 0.9.

Different marker sizes are used to represent the initial power rating. A clear pattern is detected where the smallest designs produce the worst results in all cases. These points are also associated with large flexibility spaces (larger costs). This effect is stronger for Strategy A and re-powering case (v) due to the larger initial investments. As observed previously, the baseline case and the unchangeable case (iv) exhibit a far less volatile behavior, with a clear layering given by the initial sizes. For Strategy B, even the less desirable combinations are better than those of Strategy A, due to the smaller initial costs. It is interesting to observe that the best configurations of both flexible strategies outperform the best baseline designs. This highlights the importance of finding the optimal

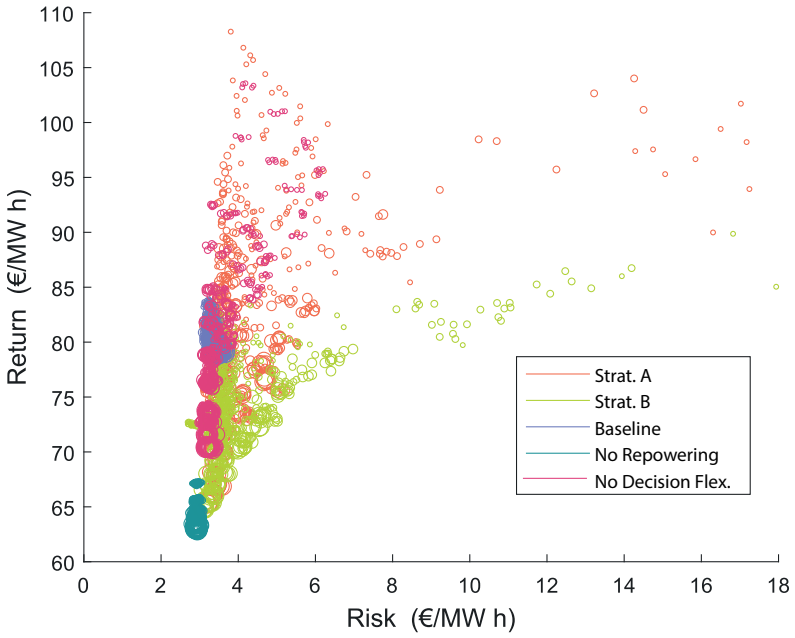

Figure 17: Risk-return space for different farm configurations and management policies

policy for each design. The optimal configurations correspond to large initial power ratings (15 - 18 MW), enough flexibility for one or two adaptations, and large AT.

These results are consistent with previous studies that suggest that large power rating turbines have a high impact on reducing energy cost [14, 13, 5]. While this measure increases turbine and platforms capital costs, other costs remain the same or change slightly, and the increment in energy produced is significant. However, the optimal configurations in Figure 17 are not an option right now due to technical limitations, even if large turbines ($>$ 12 MW) are under development. It is also not clear how the platform production costs would scale for such massive turbine sizes.

5. Conclusions

This paper proposed a methodology for modeling the life cycle performance and estimating the associated costs of flexible solutions for offshore wind turbines. The methodology is a Monte-Carlo based approach to model the response of flexible policies and design strategies to the dynamics of external processes. These processes are modeled as time series that represent uncertain parameters such as demand, capacity factor, and turbine production prices. A life-cycle cost model is used to measure the performance of flexible strategies. Two flexible design strategies were analyzed: over-dimensioned platforms and adaptable platforms, both subject to variable flexibility management policies described as functions of the external processes.

In general terms, the results showed that flexibility implemented through the adaptable platform strategy (B) can potentially be a desirable property to have in the wind farm,helping to achieve reductions in LCOE between 12 and 18% in the best cases, compared with traditionally designed floating wind farms, for operational periods of 50 years. These benefits are partially derived from

the ability of the flexible alternatives to better react to new contexts, which usually results in more energy produced at lower investments.

The cost reduction can be partially explained by the weight that production and material costs have on the total costs and, therefore, on the LCOE. By introducing flexibility to the farms, their life-cycle can be prolonged without incurring in all the initial investments required to rebuild at the end of the life-cycle while maintaining the option to deploy changes (new technologies) at a low cost.

However, flexibility not always results in cost reductions, as shown by the results of the over-dimensioned platform strategy. This strategy did not show any difference with a re-powering strategy at fixed times. When the investments required to introduce flexibility into the system are too large, the benefits may not be enough to compensate for the additional flexibility costs. Implementing flexibility requires to consider the initial investments, the future adaptation costs, the flexibility management policy, and the expected evolution of the context.

Flexibility and other lifetime extension strategies, such are re-powering, have the potential to be significant cost-reducing measures, under favorable legal frameworks. Additional research to measure not only the effect on lifetime costs but on the sustainability in general of floating offshore farms is required to understand the broad impact of flexibility. Further work is also required to explore the formulation of improved flexibility management policies.

6. Acknowledgements

This research received financial support from the Regional Council of 'Pays de la Loire' within the framework of the BUENO 2018-2021 research program (Durable Concrete for Offshore Wind Turbines) and from the Vice-rectory for Research at Universidad de los Andes.

7. References

References

[1] A. Myhr, C. Bjerkseter, A. Agotnes, T. A. Nygaard, Levelised cost of energy for offshore floating wind turbines in a life cycle perspective, Renewable Energy 66 (2014) 714–728. doi:10.1016/j.renene.2014.01.017.

[2] M. Shafiee, F. Brennan, I. Armada Espinosa, A parametric whole life cost model for offshore wind farms, International Journal of Life Cycle Assessment 21 (2016) 961–975. doi:10.1007/s11367-016-1075-z.

[3] P. Morthorst, L. Kitzing, 2 - economics of building and operating offshore wind farms, in: C. Ng, L. Ran (Eds.), Offshore Wind Farms, Woodhead Publishing, 2016, pp. 9 – 27. doi:10.1016/B978-0-08-100779-2.00002-7.

[4] R. Green, N. Vasilakos, The economics of offshore wind, Energy Policy 39 (2011) 496 – 502. doi:10.1016/j.enpol.2010.10.011, special Section on Offshore wind power planning, economics and environment.

[5] J. Bosch, I. Staffell, A. D. Hawkes, Global levelised cost of electricity from offshore wind, Energy 189 (2019) 116357. doi:10.1016/j.energy.2019.116357.

[6] B. Möller, L. Hong, R. Lonsing, F. Hvelplund, Evaluation of offshore wind resources by scale of development, Energy 48 (2012) 314 – 322. doi:10.1016/j.energy.2012.01.029, 6th Dubrovnik Conference on Sustainable Development of Energy Water and Environmental Systems, SDEWES 2011.

[7] J. Carroll, A. McDonald, I. Dinwoodie, D. McMillan, M. Revie, I. Lazakis, Availability, operation and maintenance costs of offshore wind turbines with different drive train configurations, Wind Energy 20 (2017) 361–378. doi:10.1002/we.2011.

[8] A. Ioannou, A. Angus, F. Brennan, Stochastic Prediction of Offshore Wind Farm LCOE through an Integrated Cost Model, Energy Procedia 107 (2017) 383–389. doi:10.1016/j.egypro.2016.12.180.

[9] N. Bento, M. Fontes, Emergence of floating offshore wind energy: Technology and industry, Renewable and Sustainable Energy Reviews 99 (2019) 66–82. doi:10.1016/j.rser.2018.09.035.

[10] C. Maienza, A. M. Avossa, F. Ricciardelli, D. Coiro, G. Troise, C. T. Georgakis, A life cycle cost model for flating offhore wind farms, Applied Energy 266 (2020) 114716. doi:10.1016/j.apenergy.2020.114716.

[11] J. Carroll, A. McDonald, D. McMillan, Failure rate, repair time and unscheduled O&M cost analysis of offshore wind turbines, Wind Energy 19 (2016) 1107–1119. doi:10.1002/we.1887.

[12] F. Judge, F. D. McAuliffe, I. B. Sperstad, R. Chester, B. Flannery, K. Lynch, J. Murphy, A lifecycle financial analysis model for offshore wind farms, Renewable and Sustainable Energy Reviews 103 (2019) 370–383. doi:10.1016/j.rser.2018.12.045.

[13] The Crown State, Offshore wind cost reduction, pathways study, The Crown State, 2012.

[14] M. I. Blanco, The economics of wind energy, Renewable and Sustainable Energy Reviews 13 (2009) 1372 – 1382. doi:10.1016/j.rser.2008.09.004.

[15] R. De Neufville, S. Scholtes, Flexibility in Engineering Design, Engineering systems, 1st ed., MIT Press, 2011.

[16] M. Mortazavi-Naeini, G. Kuczera, L. Cui, Application of multiobjective optimization to scheduling capacity expansion of urban water resource systems, Water Resources Research (2014) 4624–4642. doi:10.1002/2013WR014569.

[17] C. C. Fraga, J. Medellín-Azuara, G. F. Marques, Planning for infrastructure capacity expansion of urban water supply portfolios with an integrated simulation-optimization approach, Sustainable Cities and Society 29 (2017) 247–256. doi:10.1016/j.scs.2016.11.003.

[18] T. Erfani, K. Pachos, J. J. Harou, Real-Options Water Supply Planning: Multistage Scenario Trees for Adaptive and Flexible Capacity Expansion Under Probabilistic Climate Change Uncertainty, Water Resources Research 54 (2018) 5069–5087. doi:10.1029/2017WR021803.

[19] M. V. Chester, B. Allenby, Toward adaptive infrastructure: flexibility and agility in a non-stationarity age, Sustainable and Resilient Infrastructure 4 (2019) 173–191. doi:10.1080/23789689.2017.1416846.

[20] A. M. Ross, D. H. Rhodes, D. E. Hastings, Defining Changeability : Reconciling Flexibility , Adaptability , Scalability , Modifiability , and Robustness for Maintaining System Lifecycle Value, Systems Engineering 11 (2008) 246–262. doi:10.1002/sys.

[21] J. H. Saleh, G. Mark, N. C. Jordan, Flexibility : a multi-disciplinary literature review and a research, Journal of Engineering Design 20 (2009) 307–323. doi:10.1080/09544820701870813.

[22] O. Špačková, D. Straub, Long-term adaption decisions via fully and partially observable Markov decision processes, Sustain Resilient Infrastruct 2 (2017) 37–58. doi:10.1080/23789689.2017.1278995.

[23] M. Sánchez-Silva, Managing infrastructure systems through changeability, Journal of Infrastructure Systems 25 (2019) 04018040. doi:10.1061/(ASCE)IS.1943-555X.0000467.

[24] S. Torres-Rincón, D. F. Villarraga, M. Sánchez-Silva, Conceptual and Numerical Analysis of Flexibility in Infrastructure Systems, Journal of Infrastructure Systems 26 (2020) 04020012. doi:10.1061/(ASCE)IS.1943-555X.0000546.

[25] M.-A. Cardin, M. Ranjbar-Bourani, R. De Neufville, Improving the Lifecycle Performance of Engineering Projects with Flexible Strategies: Example of On-Shore LNG Production Design, Systems Engineering 18 (2015) 253–268. doi:10.1002/sys.21301.

[26] M. Fitzgerald, Managing Uncertainty in Systems with a Valuation Approach for Strategic Changeability, Master's Thesis. Massachusetts Institute of Technology, 2012.

[27] M. A. Cardin, S. Zhang, W. J. Nuttall, Strategic real option and flexibility analysis for nuclear power plants considering uncertainty in electricity demand and public acceptance, Energy Economics 64 (2017) 226–237. doi:10.1016/j.eneco.2017.03.023.

[28] W. B. Powell, Approximate Dynamic Programming: Solving the Curses of Dimensionality, 2nd ed., Wiley, 2011.

[29] S. Zhao, W. B. Haskell, M. A. Cardin, Decision rule-based method for flexible multi-facility capacity expansion problem, IISE Transactions 50 (2018) 553–569. doi:10.1080/24725854.2018.1426135.

[30] M. J. Kochenderfer, C. Amato, G. Chowdhary, J. P. How, H. J. D. Reynolds, J. R. Thornton, P. A. Torres-Carrasquillo, N. K. Üre, J. Vian, Decision Making Under Uncertainty: Theory and Application, 1st ed., The MIT Press, 2015.

[31] H. Díaz, J. M. Rodrigues, C. Guedes Soares, Preliminary cost assessment of an offshore floating wind farm installation on the galician coast, in: C. Guedes Soares (Ed.), Progress in Renewable Energies Offshore. Proceedings of the 2nd International Conference on Renewable Energies Offshore, Taylor & Francis, 2016, pp. 843–850.

[32] L. Castro-Santos, V. Diaz-Casas, Life-cycle cost analysis of floating offshore wind farms, Renewable Energy 66 (2014) 41–48. doi:10.1016/j.renene.2013.12.002.

[33] L. Castro-Santos, A. Filgueira-Vizoso, I. Lamas-Galdo, L. Carral-Couce, Methodology to calculate the installation costs of offshore wind farms located in deep waters, Journal of Cleaner Production 170 (2018) 1124 – 1135. doi:10.1016/j.jclepro.2017.09.219.

[34] L. Castro-Santos, E. Martins, C. Guedes Soares, Methodology to Calculate the Costs of a Floating Offshore Renewable Energy Farm, Energies 9 (2016) 324. doi:10.3390/en9050324.

[35] C. Mone, M. Hand, M. Bolinger, J. Rand, D. Heimiller, J. Ho, 2015 cost of wind energy review, National Renewable Energy Laboratory (NREL), 2017. doi:10.2172/1351062.

[36] E. Topham, D. McMillan, S. Bradley, E. Hart, Recycling offhore wind farms at decommissioning stage, Energy Policy 129 (2019) 698–709. doi:10.1016/j.enpol.2019.01.072.

[37] M. Sánchez-Silva, G.-A. Klutke, Relibility and Life-Cycle Analysis of Deteriorating Systems, 1st ed., Springer International, 2016.

[38] M. Duran Toksarı, Ant colony optimization approach to estimate energy demand of turkey, Energy Policy 35 (2007) 3984 – 3990. doi:10.1016/j.enpol.2007.01.028.

[39] C. García-Ascanio, C. Maté, Electric power demand forecasting using interval time series: A comparison between var and imlp, Energy Policy 38 (2010) 715 – 725. doi:10.1016/j.enpol.2009.10.007.

[40] N. Alabbas, J. Nyangon, Weather-based long-term electricity demand forecasting model for saudi arabia: A hybrid approach using end-use and econometric methods for comprehensive demand analysis, 2016.

[41] R. H. Wiser, M. Bolinger, 2011 wind technologies market report, National Renewable Energy Laboratory (NREL), 2012.

[42] The Crown State, Offshore wind operational report, The Crown State, 2019.

[43] T. Stehly, P. Beiter, P. Duffy, 2019 cost of wind energy review, National Renewable Energy Laboratory (NREL), 2020.

[44] W. Musial, P. Beiter, P. Spitsen, J. Nunemaker, V. Gevorgian, A. Cooperman, R. Hammond, M. Shields, 2019 offshore wind technology data update, National Renewable Energy Laboratory (NREL), 2020.

[45] E. Bastidas-Arteaga, M. G. Stewart, Economic assessment of climate adaptation strategies for existing reinforced concrete structures subjected to chloride-induced corrosion, Structure and Infrastructure Engineering 12 (2016) 432 – 449. doi:10.1080/15732479.2015.1020499.

[46] F. K. Crundwell, Finance for Engineers: Evaluation and Funding of Capital Projects, 1 ed., Springer Verlag, 2008.

Appendix A. Detailed Equations

Appendix A.1. Installation of turbines and platforms

The rental time of storage surface for the floating platforms $t_{sr,fp}$ $(days)$ is calculated as:

$$t_{sr,fp} = \frac{t_{ip,fp}\ n_{wt}}{24} + t_{tug,fp} \tag{A.1}$$

The assembling time of platforms at port $t_{ip,fp}$ is calculated as:

$$t_{ip,fp} = n_{li,fp}\ t_{li,fp} \tag{A.2}$$

where $n_{li,fp}$ is the number of lifting movements to assemble turbine and platform, and $t_{li,fp}$ is the time required for one lifting movement $(hours)$.

The usage time of the tug vessels $t_{tug,fp}$ is calculated $(days)$ as:

$$t_{tug,fp} = \left(n_{fp,tug}\ t_{ld,fp} + \frac{2}{3600} \frac{d_p}{v_{tug}} \right) \frac{n_{wt}}{n_{fp,tug}}\ \frac{1}{24\ k_{dt}} \tag{A.3}$$

with $n_{fp,tug}$ the number of platforms towed per trip, v_{tug} the speed of the tug vessel (m/s), d_p the distance between port and farm (m), and k_{dt} a downtime coefficient.

The rented surface at port s_{fp} is defined as:

$$s_{fp} = n_{wt}\ l_{fp}\sqrt{l_{fp}^2 - (\frac{l_{fp}}{2})^2} \tag{A.4}$$

where l_{fp} is the platform length.

Appendix A.2. Installation of electrical systems

The rental time of port surface $t_{sr,ofs}$ $(days)$ is calculated assuming that: i) a barge is used to transport the transformers to the offshore site, ii) a tug is used to tow the floating platform, and iii) a floating crane is used to assemble the substation *in situ* [10]. The parameter $t_{sr,ofs}$ is defined as the sum [33]:

$$t_{sr,ofs} = t_{b,ofs} + t_{tug,ofs} + t_{fc,ofs} \tag{A.5}$$

The barge usage time $t_{b,so}$ $(days)$ is calculated as:

$$t_{b,ofs} = \left(\frac{2}{3600}\ \frac{d_p}{v_b} + n_{ts,b}\ t_{ld,ts}\right)\frac{n_{ts}}{24\ k_{dt}} \tag{A.6}$$

with v_b the speed of the barge vessel (m/s), $n_{ts,b}$ the number of transformers transported in one barge, and n_{ofs} the number of offshore substations.

The time to load one transformer $t_{ld,ts}$ is calculated as:

$$t_{ld,ts} = n_{li,ts}\ t_{li,ts} \tag{A.7}$$

where $n_{li,ts}$ is the number of liftings to load one transformer and $t_{li,ts}$ the time required $(hours)$.

The tug usage time $t_{tug,ofs}$ is calculated as:

$$t_{tug,ofs} = \left(\frac{2}{3600}\ \frac{d_p}{v_{tug}} + n_{fp,ofs}\ t_{ld,fp}\right)\frac{n_{ofs}}{24\ k_{dt}} \tag{A.8}$$

The time to load the substation platforms $t_{ld,fp}$ is calculated as:

$$t_{ld,fp} = n_{li,fp}\ t_{li,fp} \tag{A.9}$$

The floating crane usage time $t_{fc,ofs}$ is calculated as:

$$t_{fc,ofs} = \left(\frac{2}{3600}\ \frac{d_p}{v_{fc}} + t_{is,ofs} + t_{im,fc}\right)\frac{n_{ofs}}{24\ k_{dt}} \tag{A.10}$$

with v_{fc} the speed of the floating crane (m/s) and $t_{is,ofs}$ the time between internal movement of the floating crane $(hours)$.

The installation time of the offshore substation $t_{is,ofs}$ is calculated as:

$$t_{is,ofs} = n_{li,ofs}\ t_{li,ofs} \tag{A.11}$$

The port surface s_{ofs} is defined as [33]:

$$s_{ofs} = n_{ts}(l_{ts}\ w_{ts} + l_{GIS}\ w_{GIS})(1 + 1.5) \tag{A.12}$$

with l_{ts}, w_{ts} the transformers' dimensions and l_{GIS}, w_{GIS} the GIS dimensions (m).

Appendix A.3. Estimation of adaptation costs

The rental time in *days* for the new turbines $t_{sr,wt}$ is calculated as:

$$t_{sr,wt} = t_{b,wt} + t_{pc,pa} + t_{fc,wt} \tag{A.13}$$

The barge usage time $t_{b,wt}$ is calculated as:

$$t_{b,wt} = \left(\frac{2}{3600}\ \frac{d_p}{v_b} + n_{wt,b}\ t_{ld,wt}\right) \frac{n_{wt}}{n_{wt,b}}\ \frac{1}{24\ k_{dt}} \tag{A.14}$$

with $n_{wt,b}$ the number of turbines transported per barge.

The time required to load a preassembled turbine into the vessel at port $t_{ld,wt}$ is:

$$t_{ld,wt} = n_{li,wt}\ t_{li,wt} \tag{A.15}$$

The port crane usage time for preassembly $t_{pc,pa}$ is calculated as:

$$t_{pc,pa} = \frac{n_{wt}}{24}\ (n_{li,pa}\ t_{li,pa}) \tag{A.16}$$

The floating crane usage time $t_{fc,wt}$ in *days* is calculated as:

$$t_{fc,wt} = (t_{is,wt} + t_{im,fc})\frac{n_{wt}}{24\ k_{dt}} \tag{A.17}$$

The on-site installation time of the turbines $t_{is,wt}$ is calculated according to Equation A.18:

$$t_{is,wt} = n_{li,is}\ t_{li,is} \tag{A.18}$$

The rented surface at port s_{wt} is based on the space required to store the turbines and is calculated as [33]:

$$s_{wt} = 3\ n_{wt}\ l_{bl}\ \phi_{bl} + 3\ n_{wt}\ \pi\ \left(\frac{\phi_{tw}}{2}\right)^2 \tag{A.19}$$

where l_{bl} is the length of the blades, and ϕ_{bl}, ϕ_{tw} are the diameters of the blades and the tower.